

# 자기전기복합체의 비공진 및 공진 상태에서의 자기전기 결합 특성 평가 방법

Deepak Rajaram Patil<sup>1</sup>, 류정호<sup>1,2</sup> 

<sup>1</sup> 영남대학교 신소재공학부

<sup>2</sup> 영남대학교 재료기술연구소

**초록:** 자기전기복합체(magnetolectric, ME composite)는 자왜재료와 압전재료의 결합현상을 이용하는 재료로서 지난 20여 년간 이론적, 실험적으로 많은 연구가 진행되어 왔다. 자기전기복합체의 출력특성은 구성하는 소재, 계면층, 복합체의 형상, 자기장하 진동모드 등의 많은 구성요소의 최적화를 통하여 급속히 향상되고 있다. 하지만 자기전기복합체의 자기전기 결합 특성 평가는 대부분의 연구들에서 구체적인 방법을 제시하지 않아 어떻게 측정할 것인지가 불명확한 경우가 많다. 본 논문에서는 자기전기복합체의 비공진, 공진상황에서 자기전기 전압계수를 어떻게 측정할 수 있는지에 대한 자세한 방법을 소개한다. 평가를 위한 샘플로서 대칭적인 구조를 가지는 Gelfenol/PMN-PZT/Gelfenol 자기전기복합체를 제조하였다. 압전 재료로는 이방성의 (011) 32 모드의 PMN-PZT 압전 단결정과 자왜재료로는 Galfenol 합금을 사용하여 예폭시로 접착하였다. 컴퓨터 인터페이스로 자동화된 자기전기 전압특성 측정 시스템의 구성을 우선 설명하고, 자기전기 결합특성의 측정 방법을 단계별로 설명한다. 본 튜토리얼 논문에서는 자기전기결합 특성과 특성평가방법을 이해하고자 하는 연구자들에게 도움이 될 수 있는 평가방법의 원리와 절차를 제공하고자 하였다.

**키워드:** 자기전기효과, 결합, 비공진, 공진, 복합체

## Demonstration of Magnetolectric Coupling Measurement at Off-Resonance and Resonance Conditions in Magnetolectric Composites

Deepak Rajaram Patil<sup>1</sup> and Jungho Ryu<sup>1,2</sup>

<sup>1</sup> School of Materials Science and Engineering, Yeungnam University, Gyeongsan 38541, Korea

<sup>2</sup> Institute of Materials Technology, Yeungnam University, Gyeongsan 38541, Korea

(Received April 9, 2022; Revised April 19, 2022; Accepted April 27, 2022)

**Abstract:** Magnetolectric (ME) composites are comprised of magnetostrictive and piezoelectric phases. Lots of theoretical and experimental works have been done on ME composites in the last couple of decades. The output performance of ME composites has been enhanced by optimizing the constituent phases, interface layer, dimensions of the ME composites, different operating modes, etc. However, the detailed information about the characterization of ME coupling in ME composites is not provided yet. Therefore, in this tutorial paper, we are giving an insight into the details of measurements of ME voltage coefficient of ME composites both at off-resonance and resonance conditions. A symmetric type Gelfenol/PMN-PZT/Gelfenol ME composites

✉ Jungho Ryu; [jhryu@ynu.ac.kr](mailto:jhryu@ynu.ac.kr)

Copyright ©2022 KIEEME. All rights reserved.

This is an Open-Access article distributed under the terms of the Creative Commons Attribution Non-Commercial License (<http://creativecommons.org/licenses/by-nc/3.0>) which permits unrestricted non-commercial use, distribution, and reproduction in any medium, provided the original work is properly cited.

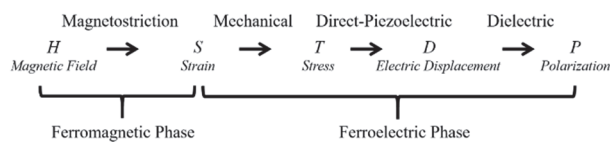
were fabricated by sandwiching (011) 32-mode PMN-PZT single crystal between two Galfenol plates by epoxy bonding are used for the example of ME coupling measurement. The details about the experimental setup used for the measurement of ME voltage coefficient are provided. Furthermore, a step-by-step measurement of ME voltage coefficient using computerized program is demonstrated. We believe the present experimental measurement details can help readers to understand the concept of ME coupling and its analysis.

**Keywords:** Magnetoelectric effect, Coupling, Off-resonance, Resonance, Composite

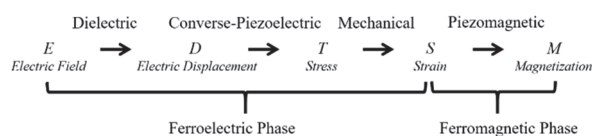
## 1. INTRODUCTION

- Magnetolectric (ME) composites comprised of magnetostrictive and piezoelectric phases possess multifunctional properties that are not present in the individual constituent phases [1-3]. The multifunctionality of these ME composites makes them potential candidates for new multifunctional devices such as sensors, transducers, energy harvesters, etc. [3-8].
- ME composites are characterized by the ME effect, which is a product property of the piezoelectric effect in the piezoelectric phase and the magnetostriction effect in the ferromagnetic phase. Depending upon the external stimuli [electric field ( $E$ ) or magnetic field ( $H$ )], there are two types of ME effects: direct ME effect (control of electric polarization  $P$  by applying  $H$ ) and converse ME effect (control of magnetization  $M$  by applying  $E$ ) [1-2].
- The direct and converse ME effects in ME composites can be easily understood from the following mechanisms.

### Direct ME effect [9]:



### Converse ME effect [9]:



- In general, the ME effect in ME composites is a strain-mediated elastic coupling between piezoelectric and magnetostrictive phases and is strongly dependent on the connectivity of the composites and interface coupling between the two phases. In the direct ME effect, the applied magnetic field induces strain in the ferromagnetic layer through the magnetostriction effect, which is then transferred as a stress to the ferroelectric phase, resulting in dielectric polarization through the direct piezoelectric effect. In the converse ME effect, the applied electric field induces stress in the ferroelectric layer through the converse piezoelectric effect, which is then transferred as a strain to the ferromagnetic phase, resulting in magnetization through the piezomagnetic effect [9].
- This tutorial mainly focuses on the direct ME effect. Different types of ME composites have been extensively investigated, according to the device application. In particular, bulk ME composites showed very large room temperature ME coupling. These composites are operated in different configurations such as L-T, T-T, and L-L (L represents longitudinal and T represents transverse) depending on the direction of  $H$  and  $P$  [10].
- The ME coupling in these composites is a product tensor property that arises due to mechanical coupling between magnetostrictive and piezoelectric phases. The magnetic-field-induced ME coupling can be represented as:

$$\alpha_{ij}^H = \left( \frac{\partial P_i}{\partial H_j} \right) = \epsilon_0 \epsilon_r \left( \frac{\partial E_i}{\partial H_j} \right) = \frac{\epsilon_0 \epsilon_r \left( \frac{\partial V}{\partial H} \right)}{t} = \epsilon_0 \epsilon_r \alpha_{ME} \quad (1)$$

- Where,  $\alpha_{ij}^H$  is the ME coefficient,  $\alpha_{ME} = \frac{1}{t} \left( \frac{\partial V}{\partial H} \right)$  is the ME voltage coefficient,  $E = (V/t)$ ,  $V$  is the voltage, and  $t$  is the thickness of the piezoelectric layer.

$\alpha$  and  $\alpha_{ME}$  are expressed in [s/m] and V/cm·Oe,

respectively. In general and simply,  $\alpha_{ME} = k \cdot d_{ij} \cdot q_{ij}$ , where  $k$  is the coupling factor between the two phases,  $d_{ij}$  is the direct piezoelectric coefficient of the piezoelectric phase,  $q_{ij}$  is the piezomagnetic coefficient, and  $q_{ij} = d\lambda_{ij}/dH$  ( $\lambda_{ij}$  is the magnetostriction of the magnetostrictive phase in the  $i$ -axis for  $H$  along the  $j$ -axis).

- In ME composites, the ME voltage coefficient,  $\alpha_{ME}$  is studied under two different conditions: off-resonance and resonance conditions. In the first condition, the  $H_{AC}$  (amplitude and frequency of the AC field) was kept constant, and  $\alpha_{ME}$  is measured as a function of  $H_{DC}$ . In the second condition, the optimized  $H_{DC}$  (at which the highest  $\alpha_{ME}$  was observed) is kept constant and  $\alpha_{ME}$  is measured as a function of the  $H_{AC}$  frequency with small amplitude (Fig. 2(c)). The  $\alpha_{ME}$  shows a 10 to 100-fold higher magnitude than that of the off-resonance  $\alpha_{ME}$  when the frequency of  $H_{AC}$  matches the electromechanical resonance (EMR) of the piezoelectric phase or the ferromagnetic resonance (FMR) of the magnetic phase in the ME composite. This paper aims to introduce the concept of ME composites, their working principles, measurement techniques, and their characterization.

## 2. EXPERIMENTAL PROCEDURE

- The ME effect in piezoelectric/magnetostrictive ME composites is preliminary based on the superior physical properties of the magnetostrictive and piezoelectric phases. Therefore, the selection of suitable constituent phases plays an important role in achieving a good ME response. Different piezoelectric materials such as AlN, BaTiO<sub>3</sub>, Pb(Zr<sub>x</sub>Ti<sub>1-x</sub>)O<sub>3</sub> (PZT), and 0.7Pb(Mg<sub>1/3</sub>Nb<sub>2/3</sub>)O<sub>3</sub>-0.3PbTiO<sub>3</sub> (PMN-PT) or Pb(Mn<sub>1/3</sub>Nb<sub>2/3</sub>)O<sub>3</sub>-PbZrTiO<sub>3</sub> (PMN-PZT) single crystals and magnetostrictive materials such as Ni, Terfenol-D, Galfenol (FeGa), and Metglas (FeCoSiB) have been widely used due to their superior physio-mechanical properties [11].
- In the present study, we have used textured Galfenol as a magnetostrictive material due to its high magnetostriction of ~400 ppm along the (100) direction under low applied magnetic fields of ~200 Oe. On the other hand, [011] oriented PMN-PZT single crystal with superior anisotropic piezoelectric

properties was used as a piezoelectric constituent. We have fabricated 2-2 type symmetric ME laminates (L-T mode) with dimensions of 10×5×1.5 mm<sup>3</sup> by sandwiching (011) 32-mode PMN-PZT single crystal (CSM1, Ceracomp Co. Ltd., Korea) between two as-machined Galfenol plates by epoxy bonding (Duralco™ 4461, Cotronics Corp, USA). The prototype of Galfenol, PMN-PZT and as-fabricated ME laminate is shown in Fig. 1(a). Prior to measuring the ME coupling properties of the samples, they were poled under an electric field of 1 kV/mm for 20 min at room temperature.

- To evaluate the ME properties of the ME laminates, the direct magnetoelectric voltage coefficient was studied at off-resonance condition ( $f=1$  kHz) as well as at resonance condition (50~250 kHz) by using the experimental setup as shown in Fig. 1(b) [12]. The experimental setup consists of a pair of Helmholtz coil, electromagnet with a DC power source, Hall probe, Tesla meter, high-speed bipolar amplifier, lock-in amplifier, and computer with ME measurement software.
- The schematic illustration of the ME coupling measurement setup is also shown in Fig. 1(c). The ME composite was loaded inside the non-magnetic Teflon sample holder with non-magnetic contact electrodes and placed between the poles of DC electromagnet superimposed with Helmholtz coil to apply DC and AC magnetic fields simultaneously along the in-plane direction of the ME composite. AC current was generated and transmitted to the Helmholtz coil through a bipolar amplifier (HSA 4011, NF Corp. Japan) which produce uniform magnetic field of 1 Oe over the frequency range of 1 kHz to 500 kHz. The exact field intensity can be calculated with an appropriate formula by measuring the driving current in the circuit. Meanwhile, DC current is delivered to the DC magnet via a DC power supply (Model- PTDP-6015-BI, POWER™ CO., Korea). A Hall probe is placed next to the ME composite sample to detect the DC magnetic field and the output of the Hall probe was measured through the tesla meter (Model 425, LakreShore, USA). The electromagnet produces the DC magnetic field in the range of ±10 kOe. The sample was connected via a BNC cable to the lock-in amplifier (SR860, Stanford Research Systems, USA) operating in the voltage differential mode to monitor the output voltage from the sample. All the instruments were interfaced to the

programmable computer software through the general-purpose interface bus (GPIB) protocol and RS-232.

- The  $\alpha_{ME}$  value was derived by dividing the output voltage ( $V_{ME}$ ) by the thickness of the PMN-PZT plate ( $t=500 \mu\text{m}$ ) and the applied  $H_{AC}$  (1 Oe at 1 kHz). For the measurement of  $\alpha_{ME}$  in the resonance condition, we swept the frequency from 50 kHz to 250 kHz at  $H_{AC}$  of 1 Oe with a background  $H_{DC}$  decided from the off-resonance ME measurement (the specific positions of the maximum  $\alpha_{ME}$  value from the off-resonance ME measurement).
- The magnetostriction measurements were carried out by the strain gauge method using strain gauges (MFLA-5-350-11, Tokyo Measuring instruments Lab.). A Magnetic field was applied parallel to the gauge to measure longitudinal magnetostrictive strain,  $\lambda_{11}$ . Impedance spectra of the laminates were measured by using an impedance analyzer (E4990A, Keysight, USA).

- The transverse ME voltage coefficient ( $H$  is applied along the length direction and  $V$  is measured along the thickness direction) was measured in the present study due to its higher magnitude than that of the longitudinal ME voltage coefficient ( $H$  along the thickness direction and  $V$  is measured along the thickness direction) [13]. To measure the ME voltage generated by ME composites we have developed a computerized program as shown in the Fig. 2.
- The ME voltage from the Galfenol/PMNPZT/Galfenol ME composite was measured for two different conditions, off-resonance (auxiliary DC sweep) and resonance conditions (frequency sweep) as shown in Fig. 2 (label 1 in Fig. 2). As can be seen in the figure, in the case of auxiliary DC sweep measurement the frequency of the ac magnetic field,  $f$  is kept constant at 1 kHz with a constant  $H_{AC}$  of 1 Oe (label 3). Both frequency and amplitude of  $H_{AC}$  can be set upon measurements.
- The ME voltage is measured as a function of  $H_{DC}$  by sweeping the  $H_{DC}$  in three different cycles. (1) from 0 to  $+H_{DC}$ , (2) from  $+H_{DC}$  to  $-H_{DC}$ , and (3)  $-H_{DC}$  to  $+H_{DC}$  similar

### 3. RESULTS AND DISCUSSION

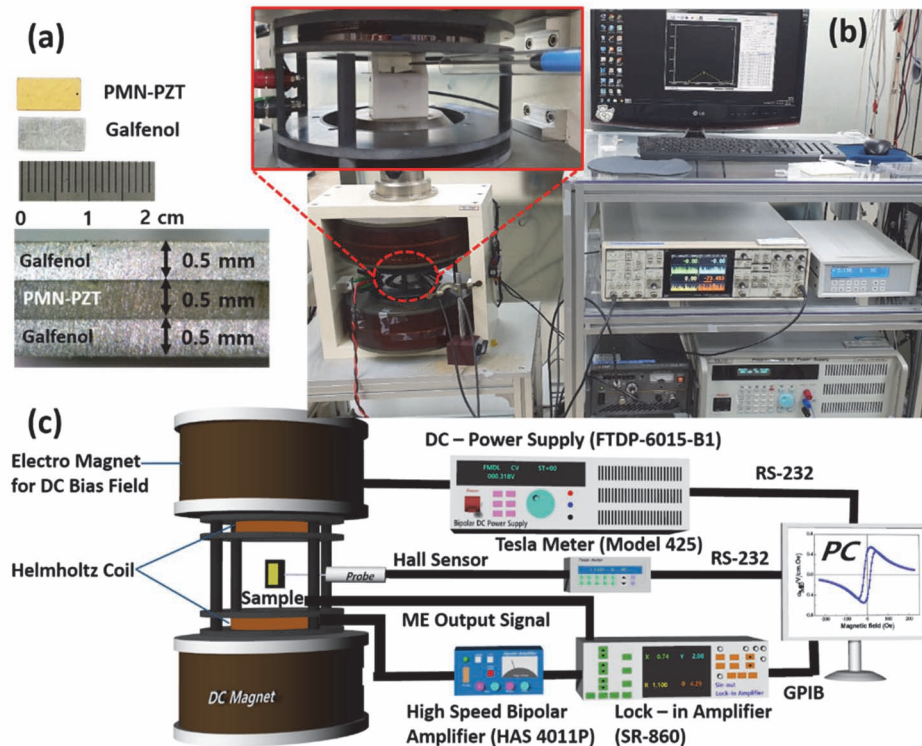


**Fig. 1.** (a) Prototype of Galfenol/PMN-PZT/Galfenol ME laminate with dimensions of  $10 (l) \times 5 (w) \times 1.5 (t)$ , (b) the real set up used for the measurement of direct ME voltage coefficient, and (c) schematic of ME set-up for the measurement of direct ME voltage coefficients [Fig. 1(a) and (c) are reproduced from ref. 12].

to magnetic hysteresis loop ( $M-H$ ) measurements. Here the magnetic field was generated by applying the DC voltage (+5 to -5 V with the number of interval steps of 201, label 2) to electromagnets in the same sequence. The interval steps in the  $H_{DC}$  were controlled by the number of steps in the applied voltage. The  $H_{DC}$  was measured using a Hall probe depending on the applied DC voltage and distance between the poles and the plot of  $V_{ME}$  for each detected field was measured and displayed in the plot as shown in Fig. 2. Different parameters such as real part ( $X$ ), imaginary part ( $Y$ ), magnitude ( $R$ ), and phase ( $\theta$ ) can be measured using a lock-in amplifier and the data can be collected by the software in real-time (label 4).

Figure 3(a) shows the variation of  $\alpha_{ME}$  as a function of applied DC magnetic field at constant  $H_{AC}$  of 1 Oe ( $f=1$  kHz).  $\alpha_{ME}$  shows a typical DC magnetic field dependence initially increases with increasing  $H_{DC}$ , attends the maximum magnitude of 0.81 V/cm·Oe at a peak field of +586 Oe, and then decreases with further increasing  $H_{DC}$ . Upon reversal of the magnetic field, it follows a similar trend with the opposite sign. The off-resonance ME effect in 2-2 structured ME laminates is expressed in terms of the ME voltage coefficient,  $\alpha_{ME}$ , which is expressed by the following equation under ideal conditions [14]:

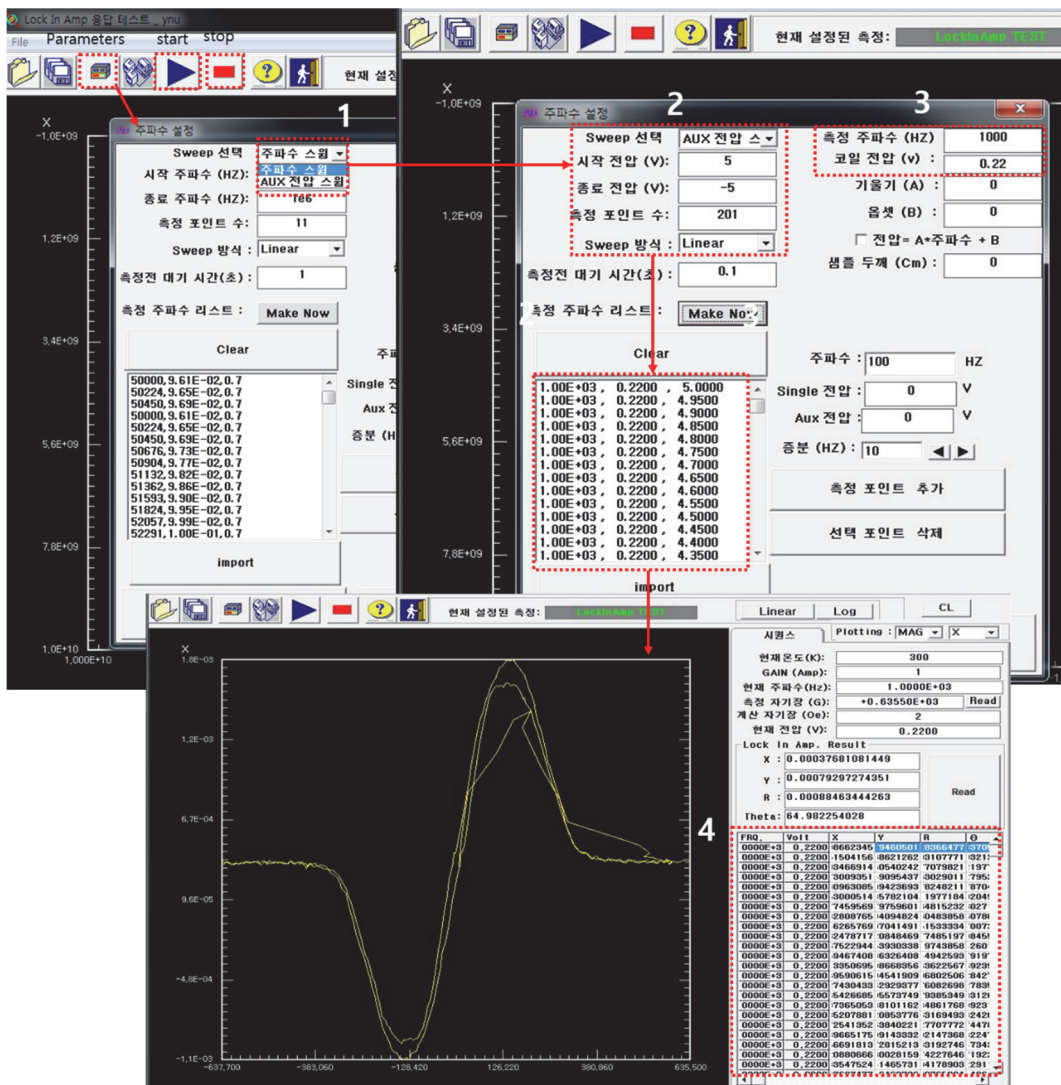
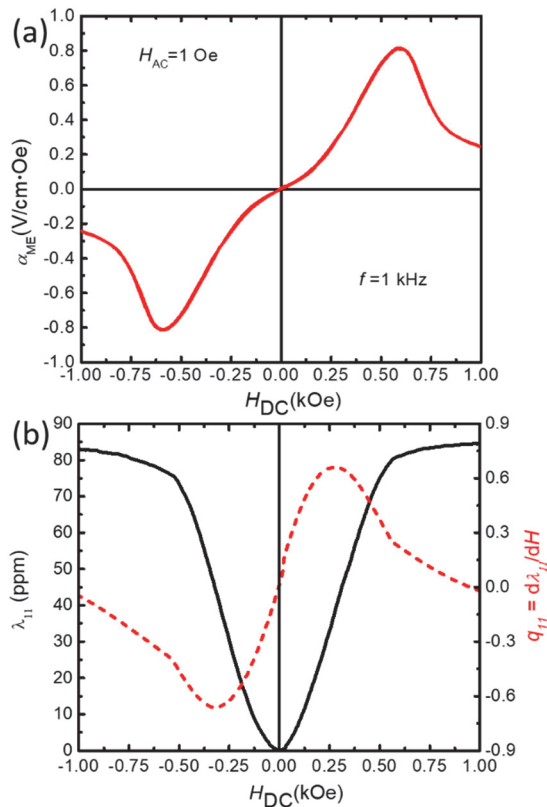


Fig. 2. Demonstration of step by step measurement of off-resonance ME voltage coefficient by using computerized program software.

$$\alpha_{ME} = \frac{-kf(1-f)d_{31}q_{11}}{(\epsilon_{33}\underline{s} - 2kf d_{31}^2)}, \quad (2)$$

Where,  $\underline{s} = f(s_{11}^p + s_{12}^p) + k(1-f)(s_{11}^m + s_{12}^m)$ . Here,  $f$  is the volume fraction of the magnetic phase;  $k$  is an interface coupling parameter ( $k = 1$  for an ideal interface and  $k = 0$  for the case without friction);  $s_{ij}^{p(m)}$  denotes the compliance for piezoelectric (magnetic) components;  $d_{31}$  (or  $d_{32}$ ) is the transverse piezoelectric coefficient;  $q_{ij}$  denotes the piezomagnetic coefficients, i.e.,  $d\lambda_{ij}/dH_j$ .

- According to the above equation, the  $H_{DC}$  dependence  $\alpha_{ME}$  is proportional to the  $H_{DC}$  dependence of the piezomagnetic coefficient  $q_{11}$ . Therefore, we measured magnetostriction of the textured Galfenol samples by applying a DC magnetic field along the longitudinal direction and calculated the corresponding  $q_{11}$  as shown in Fig. 3(b).



**Fig. 3.** (a) Transverse ME voltage coefficient ( $\alpha_{ME}$ ) of the Galfenol/PMNPZT/Galfenol ME laminates at off-resonance frequency, (b) magnetostriction ( $\lambda$ - $H$ ) and piezomagnetic coefficient ( $q$ - $H$ ) curves of the textured Galfenol (the magnetic field is applied along the length direction for the both cases).

- Figure 3(b) shows the variation of longitudinal magnetostriction ( $\lambda_{11}$ ) as a function of the DC magnetic field. The maximum  $\lambda_{11}$  for the textured Galfenol sample is found to be 82 ppm. The corresponding  $q_{11}$  was found to be positive and shows typical magnetic field dependence showing a sign change with respect to the reversal of  $H_{DC}$  direction. The magnitude of  $q_{11}$  increases initially with increasing  $H_{DC}$ , reaches a maximum of 0.23 ppm/Oe at  $H_{DC} = 280$  Oe, and then decreases with further increasing  $H_{DC}$ . From Fig. 3 it is clearly understood that both  $\alpha_{ME}(H_{DC})$  and  $q_{11}(H_{DC})$  show qualitatively and quantitatively the same magnetic field dependence.

- Next, we measured the frequency dependence of  $\alpha_{ME}$  for Galfenol/PMNPZT/Galfenol ME laminates. For the frequency dependency measurement, the frequency sweep condition was used as shown in Fig. 4 (label 1). Here, we have designed different program files for different frequency ranges which can be imported by clicking the import option (label 2). As can be seen from the figure, different program files have been written depending on the frequency ranges such as 20 Hz to 1 kHz, 1 kHz to 10 kHz, 10 kHz to 100 kHz up to 1 MHz (label 3). Each file again contains different programs based on the  $H_{AC}$  values (from 0.0001 Oe to 1 Oe) with the different number of frequency sweep steps (label 4).

- Because the Helmholtz coil has inductor behavior, the impedance of the Helmholtz coil varies with driving frequency, thus the driving voltage for Helmholtz coil should be carefully adjusted depending on the impedance of the Helmholtz coil with frequency. In our case, the impedance of the Helmholtz coil was measured with various frequency ranges when set-up the characterization system initially, and the measurement condition input file is prepared accordingly.

- Depending upon the dimensions and vibrational mode of the ME composite (e.g. bending or longitudinal vibration modes) we can choose the frequency ranges given in the program input files.

- After selecting the desired program input files, we run the program by clicking the run option (label 5). Here, the Aux voltage (label 6) for DC bias field was chosen from the Fig. 3(a), which corresponds to the optimized  $H_{DC}$  where  $\alpha_{ME}$  shows maximum value.

- The frequency measurement result is shown in Fig. 5(a). We swept the frequency from 50 kHz to 250 kHz under a constant bias field of 586 Oe [maximum value of  $\alpha_{ME}$  in Fig. 3(a)].  $\alpha_{ME}$  showed a single resonance peak at 138 kHz

with maximum magnitudes of 26.75 V/cm·Oe which is about 33 times higher than that observed at off-resonance frequency of 1 kHz [Fig. 3(a)]. The resonance occurs when the frequency of  $H_{AC}$  matched the electromechanical resonance (EMR) of the piezoelectric phase in the ME composite. The resonance peak observed at 138 kHz is attributed to the 32-vibrational mode of PMN-PZT along the length direction and can be given derived from [15],

$$f_r = \frac{1}{2l} \sqrt{\left(\frac{1-\nu}{s_{11}^p} + \frac{\nu}{s_{11}^m}\right) / \bar{\rho}} \quad (3)$$

where,  $l$  is the length of the ME laminate,  $\nu$  – volume

fraction of the magnetostrictive phase and  $\bar{\rho} = \nu\rho_m + (1 - \nu)\rho_p$  is the average mass density, where  $\rho_p$  and  $\rho_m$  represent the densities of the PMN-PZT and Galfenol, respectively.  $s_{11}^p$  and  $s_{11}^m$  are the elastic compliance coefficients of the PMN-PZT and Galfenol, respectively.

- The origin of the resonance frequency of ME composites can be understood from the impedance spectrum of the composite. Therefore, we measured the impedance spectrum of the ME composite by using an impedance analyzer as shown in Fig. 5(b). From the impedance spectrum, it is evident that  $\alpha_{ME}$  is maximum at the frequency, which is corresponding to the anti-resonance frequency ( $f_a$ ) in the impedance spectrum.

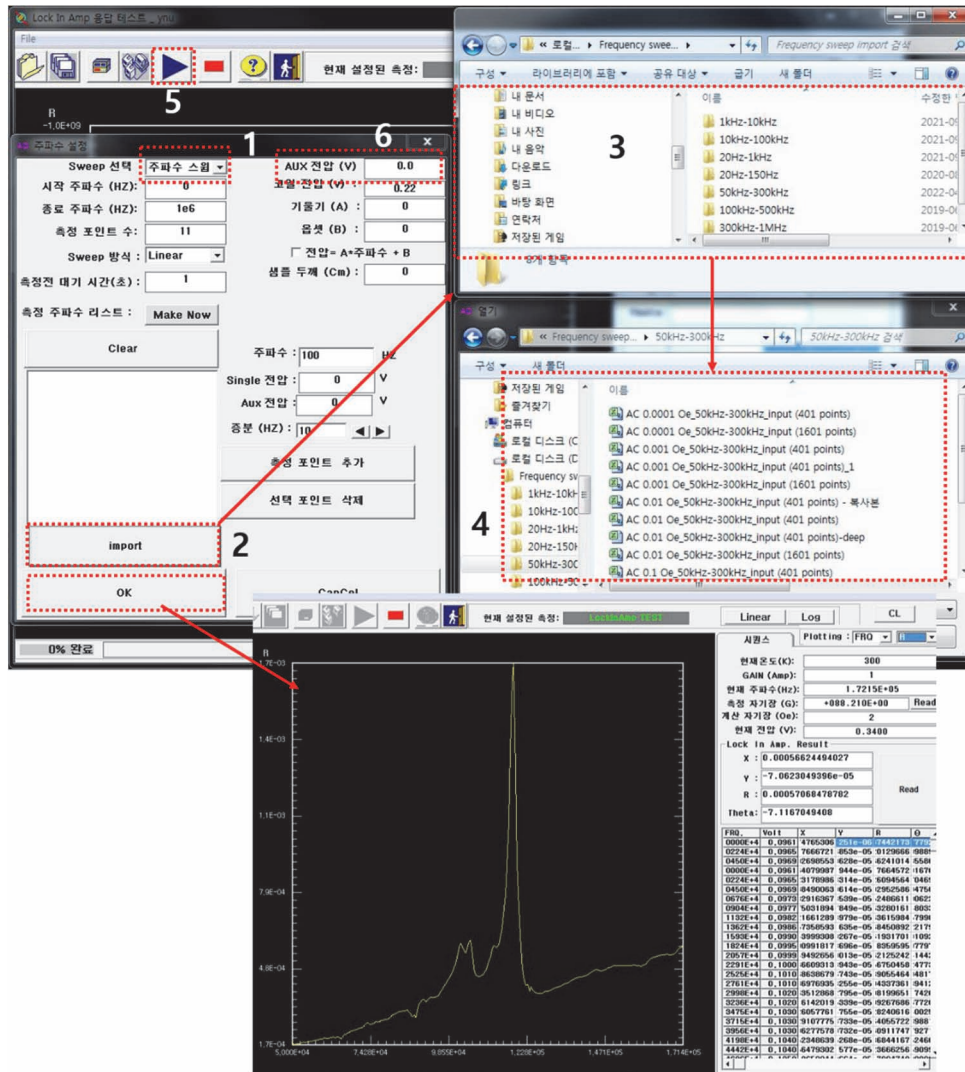
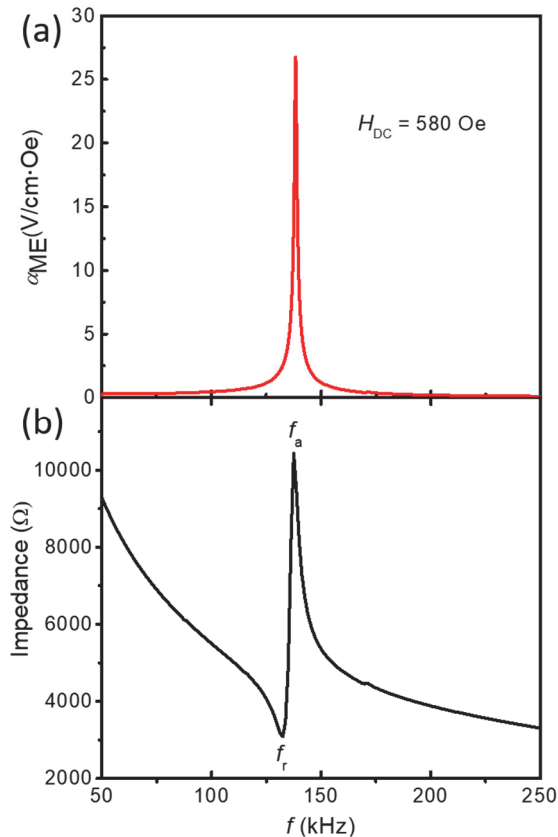


Fig. 4. Demonstration of step by step measurement of frequency dependent ME voltage coefficient by using computerized program software.



**Fig. 5.** (a) Transverse ME voltage coefficient ( $\alpha_{ME}$ ) as a function of frequency for the Galfenol/PMNPZT/Galfenol ME composite and (b) impedance spectra of Galfenol/PMNPZT/Galfenol ME composites indicating resonance ( $f_r$ ) and anti-resonance frequencies ( $f_a$ ) ( $\alpha_{ME}$  is maximum at  $f_a$ ).

- These features can be understood from the piezoelectric conversion mechanism of the piezoelectric layer. At anti-resonance frequency ( $f_a$ ), the direct piezoelectric energy conversion is enhanced, thereby maximizing direct ME voltage coefficient while at resonance frequency ( $f_r$ ), the converse piezoelectric energy conversion is enhanced, thereby maximizing converse ME voltage coefficient. [9]

#### 4. CONCLUSIONS

- The present tutorial provides the details of the measurement of the ME voltage coefficient in ME composites both at off-resonance and resonance conditions. The symmetric type Galfenol/PMN-PZT/Galfenol ME composites were fabricated by sandwiching (011) 32-mode PMN-PZT

single crystal between two Galfenol plates by epoxy bonding for demonstration.

- The details of the experimental setup used for the measurement of the ME voltage coefficient are provided. Furthermore, step-by-step measurement of ME voltage coefficient using a computerized program is explained. We believe the present experimental measurement details of the ME voltage coefficient can help readers to understand the concept of ME coupling and its analysis.

#### ORCID

Jungho Ryu

<https://orcid.org/0000-0002-4746-5791>

#### 감사의 글

본 연구는 글로벌프론티어/하이브리드 인터페이스 기반 미래소재연구사업(NRF-2016M3A6B1925390)의 지원으로 수행되었습니다.

#### REFERENCES

- J. Ryu, A. V. Carazo, K. Uchino, and H. E. Kim, *Jpn. J. Appl. Phys.*, **40**, 4948 (2001). [DOI: <https://doi.org/10.1143/JJAP.40.4948>]
- J. Ryu, S. Priya, K. Uchino, and H. E. Kim, *J. Electroceram.*, **8**, 107 (2002). [DOI: <https://doi.org/10.1023/A:1020599728432>]
- V. Annapureddy, H. Palneedi, W. H. Yoon, D. S. Park, J. J. Choi, B. D. Hahn, C. W. Ahn, J. W. Kim, D. Y. Jeong, and J. Ryu, *Sens. Actuators, A*, **260**, 206 (2017). [DOI: <https://doi.org/10.1016/j.sna.2017.04.017>]
- C. M. Leung, J. Li, D. Viehland, and X. Zhuang, *J. Phys. D: Appl. Phys.*, **51**, 263002 (2018). [DOI: <https://doi.org/10.1088/1361-6463/aac60b>]
- M. G. Kang, R. Sriramdas, H. Lee, J. Chun, D. Maurya, G. T. Hwang, J. Ryu, and S. Priya, *Adv. Energy Mater.*, **8**, 1703313 (2018). [DOI: <https://doi.org/10.1002/aenm.201703313>]
- W. Kleemann, *J. Phys. D: Appl. Phys.*, **50**, 223001 (2017). [DOI: <https://doi.org/10.1088/1361-6463/aa6c04>]
- A. V. Turutin, J. V. Vidal, I. V. Kubasov, A. M. Kislyuk, M. D. Malinkovich, Y. N. Parkhomenko, S. P. Kobeleva, A. L. Kholkin, and N. A. Sobolev, *J. Phys. D: Appl. Phys.*, **51**, 214001 (2018). [DOI: <https://doi.org/10.1088/1361-6463/aabda4>]
- J. Ryu, J. E. Kang, Y. Zhou, S. Y. Choi, W. H. Yoon, D. S. Park, J. J. Choi, B. D. Hahn, C. W. Ahn, J. W. Kim, Y. D. Kim, S. Priya, S. Y. Lee, S. Jeong, and D. Y. Jeong, *Energy Environ.*

- Sci.*, **8**, 2402 (2015). [DOI: <https://doi.org/10.1039/C5EE00414D>]
- [9] K. H. Cho and S. Priya, *Appl. Phys. Lett.*, **98**, 232904 (2011). [DOI: <https://doi.org/10.1063/1.3584863>]
- [10] J. Ma, J. Hu, Z. Li, and C. W. Nan, *Adv. Mater.*, **23**, 1062 (2011). [DOI: <https://doi.org/10.1002/adma.201003636>]
- [11] H. Palneedi, V. Annapureddy, S. Priya, and J. Ryu, *Actuators*, **5**, 9 (2016). [DOI: <https://doi.org/10.3390/act5010009>]
- [12] H. Song, M. Peddigari, A. Kumar, S. Lee, D. Kim, N. Park, J. Li, D. R. Patil, and J. Ryu, *J. Alloys Compd.*, **834**, 155124 (2020). [DOI: <https://doi.org/10.1016/j.jallcom.2020.155124>]
- [13] D. Patil, J. H. Kim, Y. S. Chai, J. H. Nam, J. H. Cho, B. I. Kim, and K. H. Kim, *Appl. Phys. Express*, **4**, 073001 (2011). [DOI: <https://doi.org/10.1143/apex.4.073001>]
- [14] D. R. Patil, Y. Chai, R. C. Kambale, B. G. Jeon, K. Yoo, J. Ryu, W. H. Yoon, D. S. Park, D. Y. Jeong, S. G. Lee, J. Lee, J. H. Nam, J. H. Cho, B. I. Kim, and K. H. Kim, *Appl. Phys. Lett.*, **102**, 062909 (2013). [DOI: <https://doi.org/10.1063/1.4792590>]
- [15] D. R. Patil, R. C. Kambale, Y. Chai, W. H. Yoon, D. Y. Jeong, D. S. Park, J. W. Kim, J. J. Choi, C. W. Ahn, B. D. Hahn, S. Zhang, K. H. Kim, and J. Ryu, *Appl. Phys. Lett.*, **103**, 052907 (2013). [DOI: <https://doi.org/10.1063/1.4817383>]